La Metallurgia Italiana
International Journal of the Italian Association for Metallurgy

A study of intermetallic phase stability in Al-Si-Mg casting alloy: the role of Cu additions

E. Cerri, M.T. Di Giovanni, E. Ghio

The influence of Cu content (0, 0.5 and 1 wt%) on the nature of intermetallic phases was carefully investigated in a AlSiMg casting alloy. Four different Cu-bearing phases, with a Cu content ranging from 5% to 30%, were identified by Energy Dispersive Spectroscopy. The Al-Mg-Si-Cu quaternary phase was found coupled to Si particles and the Θ-Al_2Cu to brittle β-Al_5SiFe phase. Copper modified the stability and the dissolution kinetics of iron-bearing intermetallics (π-$Al_8FeMg_3Si_6$ and β-Al_5SiFe) during solution treatments at 773 and 803 K (500 and 530 °C). In 0% Cu and 0.5% Cu samples, (β+ π) area fraction decreases with time, while it remains almost constant and comparable at the end of two solution treatments in 1% Cu samples. Moreover, the Q-$Al_5Cu_2Mg_8Si_6$ and Mg_2Si intermetallic area fraction increased with copper (in 0.5 and 1% Cu samples) especially at the highest temperature of investigation (803 K - 530°C) and slightly decreased with time.

KEYWORDS: INTERMETALLIC PHASE; METALLOGRAPHIC TECHNIQUE; MECHANICAL PROPERTIES; HEAT TREATMENT.

INTRODUCTION

The high strength to weight ratio, the high thermal conductivity and the excellent castability make the Al–Si hypoeutectic alloys perfect candidates for the automotive industry. Nevertheless, in order to address the demanding requirements of the engine components, the alloy strengthening can be achieved by performing solution heat treatment and subsequent age hardening. Alloying elements like Copper (Cu) and Magnesium (Mg) are often added to this class of alloys for these purposes. While a fraction of these elements, due to their appreciable solubility, strengthens the Al-α matrix through solid solution strengthening, the remaining forms the Cu/Mg eutectic bearing phases (Θ-Al_2Cu, Q-$Al_5Cu_2Mg_8Si_6$ and π-$Al_8FeMg_3Si_6$) [1,2]. These phases appear at the last stages of solidification and hence, they can be reduced or partially dissolved by an appropriate solution heat treatment. Afterwards, atom elements may be engaged for the precipitation to induce finely distributed metastable phases that strengthen the alloys [3,4]. Solution treatment effectiveness depend on the nature of the diffusing atoms, on SDAS spacings, on the temperature and on time expo-

E. Cerri, M.T. Di Giovanni, E. Ghio
Dept. Engineering and Architecture, University of Parma, v. G. Usberti 181/A, 43124 - Parma (ITALY)
corresponding author: emanuela.cerri@unipr.it

sure [5]. The intermetallic particles formed during solidification show different tendency to dissolve; while ε-Mg_2Si and Θ-Al_2Cu phases are generally easy to dissolve, the Q-$Al_5Cu_2Mg_8Si_6$ is usually reported to be rather stable during solution treatment. Further, Fe-rich phases such as the α-$Al_{15}(Fe, Mn)_3Si_2$ phase or the typical needle like β-Al_5FeSi, undergo gradual dissolution only after long term solution treatment at high temperature [6]. The π-$Al_6Mg_3FeSi_6$, depending on the Mg fraction, may evolve to form the β-Al_5FeSi phase. In particular the transformation is faster with low Mg content, while for 0.6-0.7 wt% Mg, the process may be inverted, leading to the formation of π-$Al_6Mg_3FeSi_6$ from the β-Al_5FeSi [7-9].

It has also been found that those intermetallics may be insoluble/ partially soluble depending on the Mg/Cu fraction [10]. An interesting study proposed by Zheng et al. [11] reported that the high Cu/Mg ratio promotes the formation of Θ-phase and Q-phase. In the case of low Cu/Mg ratio promotes the formation of Mg_2Si, while under the same Cu/Mg ratio the high content of Cu and Mg simultaneously induces the formation of Θ-phase and Q-phase. In case these intermetallic phases do not dissolve during solution treatment, the strengthening effect of the Cu and Mg elements will be less efficient and the ductility of the alloys will suffer too [12]. In this concern, to reduce the un-dissolved Cu-Mg intermetallic compounds, Javidani et al. proposed an optimized Cu-Mg content ratio [13]. Another interesting contribute was proposed by L. Lasa [14]. The study combined metallographic analysis with differential scanning calorimetry (DSC) to investigate the evolution of the Cu and Mg bearing phases in hypereutectic Al-Si-Cu-Mg casting alloys.

To the knowledge of the authors, there exist only few papers on the influence of the solution heat treatment on the Mg/Cu bearing compounds in an A356 alloy with and without Cu addition. Therefore, a comprehensive investigation based on microhardness tests, quantitative metallography and electric conductivity measurements has been performed to explore the evolution of the main intermetallic phases over different solution treatment temperature and holding times.

MATERIALS AND METHODS

A Sr-modified A356 alloy was used as base material for investigations. The alloy was melted in a boron-nitride coated clay-graphite crucible at 1023 K (750 °C) and grain refined by means of Al-5Ti-1B master alloy additions. Cu was added to the melt in form of pure copper grains according to the targeted nominal concentrations of 0.5 and 1 wt% to obtain two Cu modified alloys. Molten metal was successively stirred and allowed to settle for 30 min to ensure complete dissolution of the grain refiner. Alloys were then degassed with argon gas for 5 min just prior to be poured in a copper mold of 60x100x40 mm. The temperature of the die was kept at 323 K (50 °C) during the casting trials. Samples from the three different melts (0%Cu, 0.5%Cu and 1%Cu) have been obtained and analysed by optical emission spectroscopy (OES). Their chemical compositions and alloy codes are given in Tab. 1.

Tab.1 - Chemical composition (wt%) of A356 reference alloy and Cu-containing alloys as measured by OES together with their classification [13].

Alloy	Si	Mg	Fe	Cu	Ti	B	Sr	Al	Code
A356 (Reference)	6.62	0.22	0.09	0.01	0.10	4.6 ppm	14 ppm	Bal.	Cu0
A356 + 0.5wt%Cu	6.59	0.26	0.08	0.45	0.10	5.6 ppm	80.8 ppm	Bal.	Cu0.5
A356 + 1wt%Cu	6.91	0.26	0.09	0.98	0.09	5.6 ppm	74.5 ppm	Bal.	Cu1

The alloys were solution treated in an air circulating electrical furnace at temperatures of (773±5)K (S500°C) and (803±5)K (S530°C) for times ranging from 1 h up to 12 h and then quenched in water at 293K.

Vickers microhardness (HV) was measured on each sample with a load of 500 g for a dwell time of 15 s. Microhardness indentations were also performed on the polished α-aluminium matrix with a load of 5g to estimate any solid solution strengthening during solution treatment. Each plotted value represents the average of 10 measurements

(± the standard deviation). Electrical conductivity measurements, based on Eddy current, were also performed on treated samples by using a Foerster Sigmatest operating at 60 kHz, to integrate data obtained by microindentation results.

For microstructure investigations, samples were mechanically grinded by SiC papers and polished with colloidal silica suspension. With the aim of enhancing the contrast between the Mg bearing phase (π) and the Cu intermetallics (Q), samples were etched by a fresh prepared solution of 3 ml HNO_3 in 100 ml H_2O [13]. Optical microscopy (OM) was performed with a LEICA DMi8 inverted light microscope equipped with LAS image analysis software for quantitative metallography. According to the ISO 13322-1:2014 British Standard [16], a measurement field was systematically defined over each sample. It included 20 measurement frames, each of ~ 10643.5 μm² (at a magnification of 1000X). The total investigated area was ~ 212896.6 μm². Details of the procedure are reported in [17]. Area Fraction of the particles (Af %) has been selected as key parameters. Uncertainty (error) has been estimated by encompassing two main contributions: one related to the operator and one to the instrument (constant value). To do that, an image generator software created a reference image containing 20 different objects of known dimension and then, the reference image was artificially blurred in order to reproduce the worst possible real case. Afterwards, blurred image objects were measured 10 times using the settled procedure and the resulting standard deviation was referred as uncertainty. Phases distinguished by chemical etching with OM were checked and identified through energy dispersive X-ray spectroscopy (EDS) in a FEG-SEM microscope.

RESULTS AND DISCUSSION

As-cast Microstructure

The typical microstructure features of the investigated alloys in the as-cast state are presented in Fig. 1.

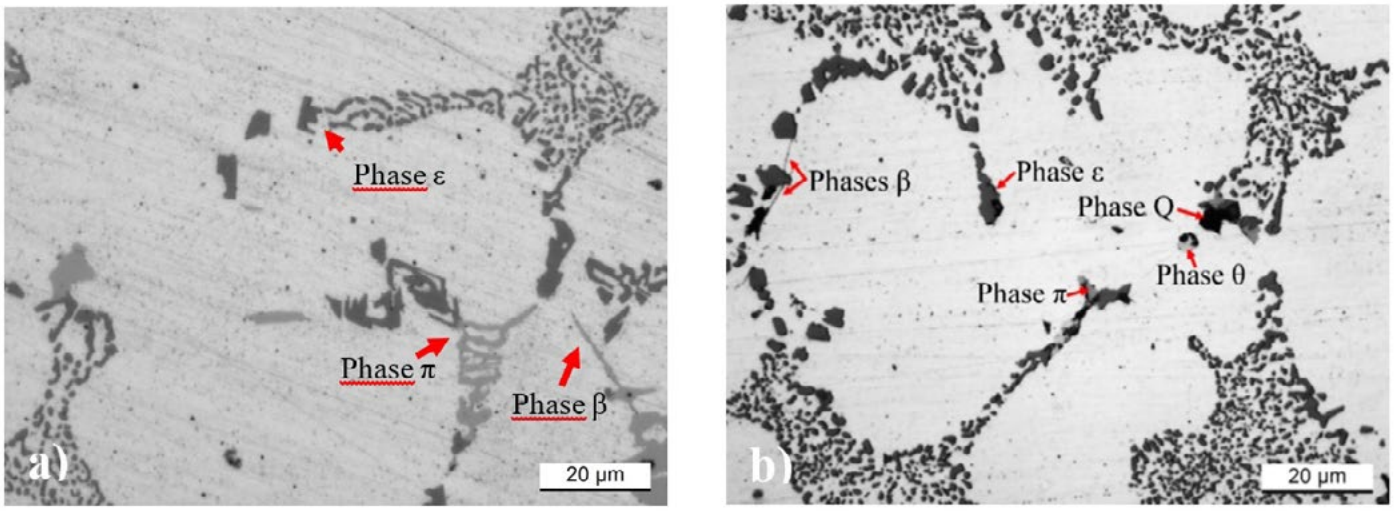

Fig.1 - Micrograph of the as-cast sample with a) 0 and b) 1 wt % Cu. Q-$Al_5Cu_2Mg_8Si_6$ phases are found in black colour, θ-Al_2Cu phase appears as the brightest phase; β-Al_5FeSi and π-$Al_8FeMg_3Si_6$ intermetallics are in light grey. The 'ε' phase is Mg_2Si.

Fig. 1a shows the micrographs of the Cu0 sample and Fig. 1b refers to the Cu1 as-cast one. The etchant developed by [13] was applied in order to discriminate the two Mg-containing intermetallic compounds, Q-$Al_5Cu_2Mg_8Si_6$ and π-$Al_8FeMg_3Si_6$, which usually appear of similar color (light gray) and morphology. As shown in Fig. 1, Q-phases are found in black color after etching according to sub sections "Microstructure study by optical and scanning electron microscopy" and " Area fraction of the investigated phases", θ-Al_2Cu phase appears as the brightest phase and β-Al_5FeSi intermetallic is recognizable by its characteristic lamellar morphology. The 'ε' phase in the following pictures has to be considered as Mg_2Si. Further insights about the phases are discussed by the authors in ref. [15].

Evolution of Hardness

Fig. 2 shows the Vickers hardness evolution of the three alloys as function of time for different heat treatment

conditions. Fig. 2a and 2b illustrate the results of the solution heat treatments at 773 K (S500°C) and 803 K (S530°C) respectively; Fig. 2c and 2d report the results for samples heat treated at high temperatures followed by natural aging for one year at room temperature (S500°C+NA and S530°C+NA respectively).

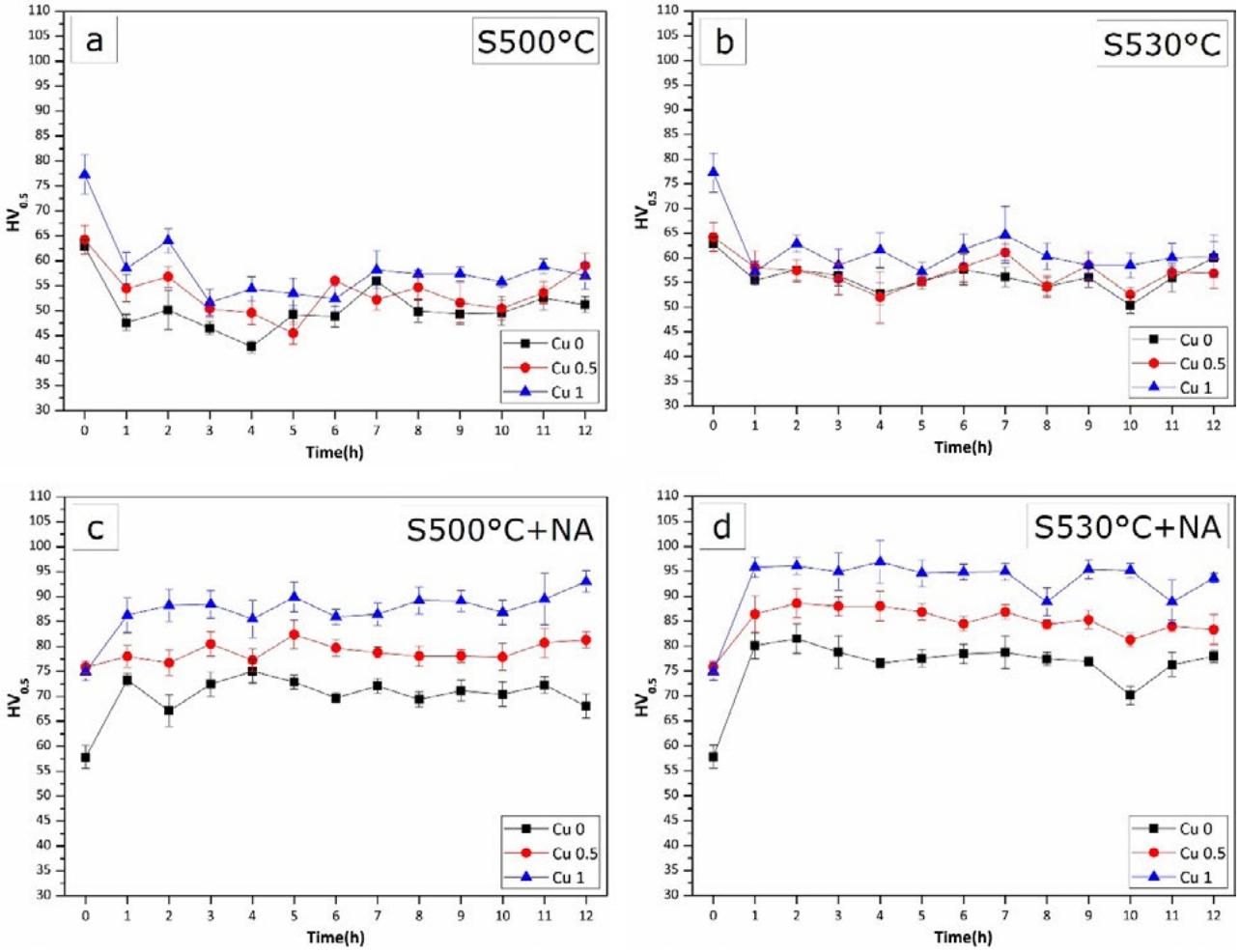

Fig.2 - Micro-hardness (HV) evolution with time during different heat treatments for alloys with different Cu content. a) Solution heat treated at 500°C (S500°C); b) solution heat treated at 530°C (S530°C); c) sol. heat treated at 500°C + naturally aged for 1 year (S500°C+NA); d) sol. heat treated at 530°C + naturally aged for 1 year (S530°C+NA).

It can be seen that the chemical composition has a strong influence on the hardness values. The increase in Cu content results, as many researchers stated [18-20], in an overall hardness enhancement, as more atoms go into the solid solution. HV curves (Figs. 2a and b) reflect the coexistence of two counteracting phenomena: on one side there is the spheroidization and the coarsening of the Si-particles responsible for the initial decay in hardness (see Silicon particles in Figs. 4 and 5) and, on the other side, there is the solid solution strengthening promoted at high temperature, more pronounced in S530°C samples. After exposure at room temperature for twelve months (Figs. 2c and 2d), the aging response is comprehensive of all the mechanisms responsible for strengthening, in particular: i) α-matrix precipitates and, ii) Si particles and intermetallic compounds. As consequence of the slow and long time aging at room temperature, hardness curves in Figs. 2c and 2d offer greater stability as compared to those in Figs. 2a and 2b referred to the solution treated samples. The shift observed between the Cu0, Cu0.5 and Cu1 alloys is mainly imputable to the density increase of the metastable Mg_2Si phase (designed as 'ε' in this paper), to precipitation of Q' and Θ'' and to Cu remaining in solid solution [21]. The effect of precipitation strengthening is more efficient for the S530°C+NA samples and increases with Cu content as shown in Fig. 3, where the ΔHV is the incremental difference between hardness average values after natural aging and just solution treated at 500° and 530°C.

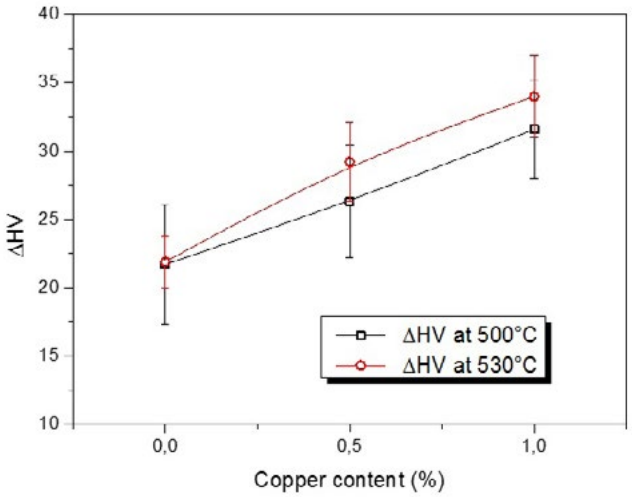

Fig.3 - Incremental difference (ΔHV) between average HV values after one year natural aging and in the as solution treated state at 500°C and 530°C, as function of Cu content in the alloys.

Despite what mentioned above, a relevant hardness contribution might be attributed to eutectic Si and intermetallic compounds evolution and/or modification and/or dissolution. In particular, in order to assess the solubility/stability of these phases and hence correlate the mechanical response, four representative points have been selected for image analysis investigations in the three Cu content alloys over the two heat treatment conditions: 0h, 4h, 5h, 12h in S500°C+NA state and 0h, 4h, 8h and 12h S530°C+NA condition.

Microstructure study by optical and scanning electron microscopy

Aiming to validate the efficiency of the proposed etching, and hence to perform image analysis by means of optical micrographs, a comparison between the as-cast and the heat treated case have been offered in Figs. 4 and 5, respectively.

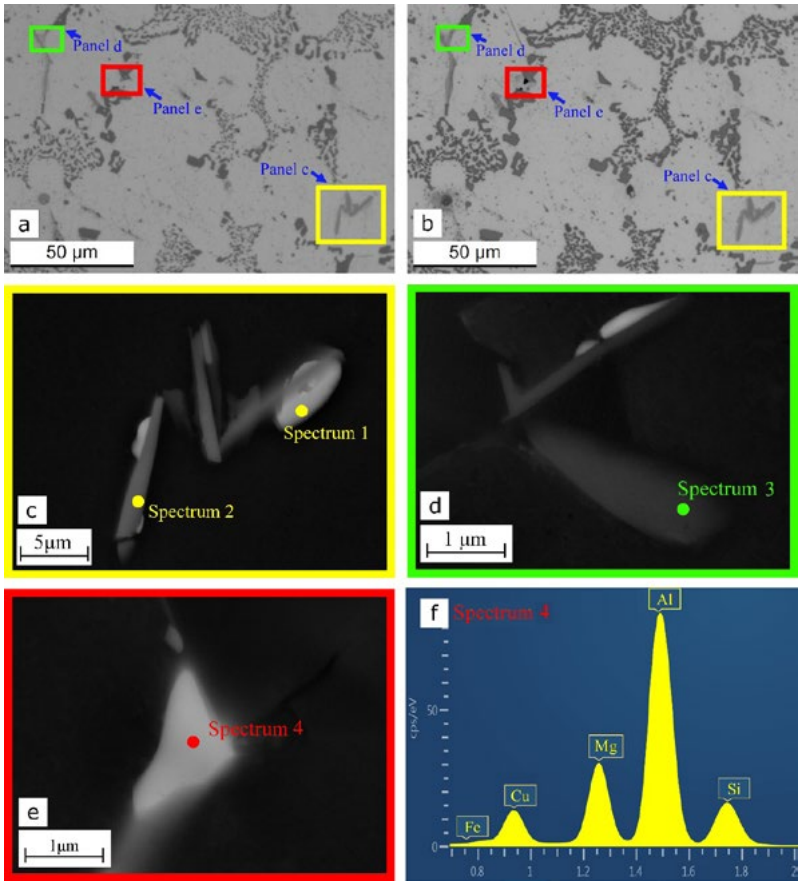

Fig.4 - BSE images of the Cu1 as-cast sample a) before and b) after chemical etching. c), d) and e) High magnification BSE images of the detected phases; f) Q-phase EDS spectrum.

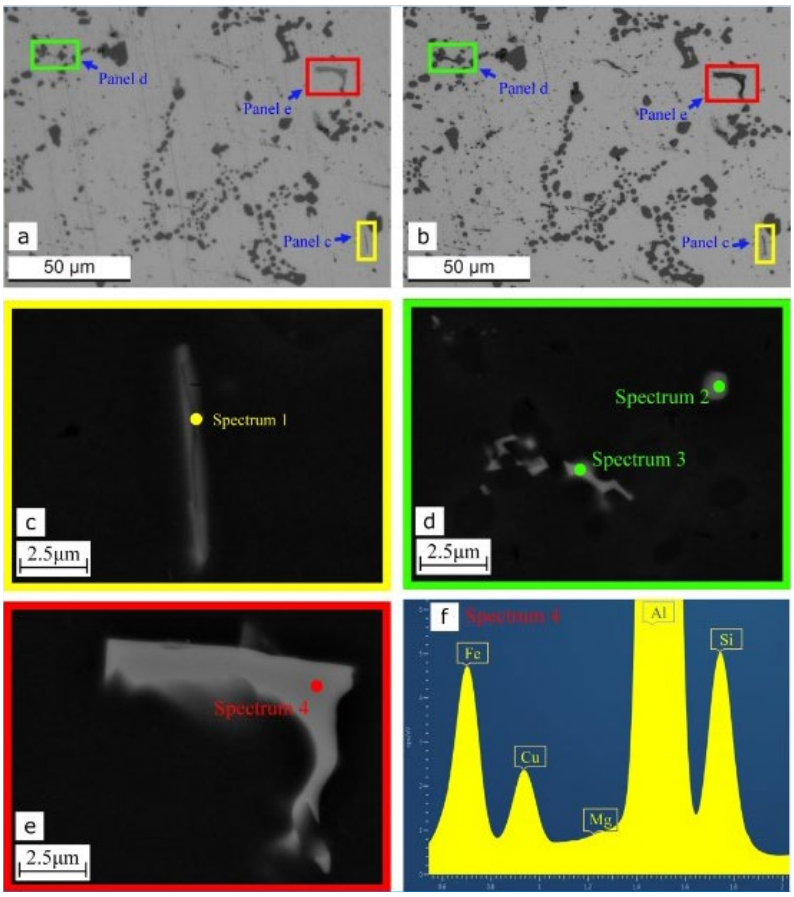

Fig.5 - BSE images of the Cu1 sample, solution heat treated at 500°C for 4 h, a) before and b) after chemical etching. c), d) and e) High magnification BSE images of the detected phases; f) EDS spectrum #4.

The micrographs of the as-cast Cu1 alloy before and after etching are shown in Figs. 4a and 4b, respectively. Three representative intermetallic compounds were marked by squares and further investigated with the help of backscattered electron (BSE) images and EDS spectra (Fig. 4c, d, e and 4f respectively). Their chemical compositions as measured by semi-quantitative EDS analysis are labelled in Table 2.

Tab.2 - Chemical composition of the intermetallic phases shown in Fig. 4. measured by semi-quantitative EDS analysis.

Spectrum	Phases	Al (%)	Mg (%)	Si (%)	Fe (%)	Cu (%)	Tot. (%)
Panel c	1	Θ	66.17	0.53	1.64	29.89	100.00
Panel c	2	β	81.7	0.23	10.27	0.52	100.00
Panel d	3	π	68.08	9.05	19.82	-	100.00
Panel e	4	Q	59.81	17.68	17.3	5.15	100.00

Q and Θ phases are found in Fig. 4c to be coupled with small and isolated β-plates, as also observed by [22]. With reference to Fig. 4a and 4b, EDS measurements (Table 2 and Fig. 4) confirm the selective nature of the applied etching: the Q-phases are preferentially etched compared to others. In Fig. 4d, the π- phase is found together with the β-phase. The spectrum in Fig. 4d related to the π-phase shows as the concurrent content of Mg, Si and Fe prevents the reactivity of this compound to the proposed etching (Figs. 5a and b), allowing us to discriminate the two Mg-rich phases under OM. Finally, Figs. 4e and 4f show a BSE image of a Q-phase and its spectrum respectively, firstly displayed in Fig. 4a and Fig. 4b

and marked with panel "e". After chemical etching by HNO_3, the Q-phase changes to black colour; the same scenario was observed in the work proposed by Javidani [4]. In addition, the author reported an excellent agreement between the results of OM and X-ray elemental mapping (EPMA) to distinguish the phases.

In analogy to the as cast case (Fig. 4), Fig. 5 shows BSE micrographs of the sample with 1 wt% Cu solution treated at 773 K (S500°C) for 4h. With reference to the Figs. 5a and 5b, the phases indicated with "d" and "e" panels reveal their susceptibly to the etching, contrary to the β-phase indicated with "c" panel and further investigated in Fig. 5c. Focusing now on the compositions of the detected phases (Figs. 5c, d, e) labelled in Table 3, it is possible to observe a new phase (as compared to the as-cast case), listed as Al-Si-Cu-Fe and previously reported by [22].

Tab.3 - Composition of the Intermetallic phases reported in Fig. 5. as measured by semi-quantitative EDS.

Spectrum		Phases	Al (%)	Mg (%)	Si (%)	Fe (%)	Cu (%)	Tot. (%)
Panel c	1	β	85.55	0.30	4.58	8.63	0.94	100.00
Panel d	2	Al-Si-Cu-Fe	76.58	0.16	8.17	12.34	2.75	100.00
Panel d	3	Al-Si-Cu-Fe	79.79	0.23	7.59	9.88	2.51	100.00
Panel e	4	Al-Si-Cu-Fe	80.8	0.26	7.43	9.28	2.23	100.00

Performing image analysis over different samples in the as-cast and heat-treated conditions, black phases were accounted as Q-phase and/or eventually Mg_2Si phase. Thought apparently, during the solution treatment this Mg- and Cu-rich compound seems to loose almost integrally its Mg content and partially its Si-content, while getting enriched in Fe. Javidani in [4] demonstrated that the stability of Q-phase is strictly dependent of the Cu/Mg ratio, and in details the alloys with lower Cu content (1.5 wt.% Cu and ~0.3 wt. % Mg) experience the dissolution of this phase at ~803K (530°C).

Area fraction of the investigated phases

The measured area fraction of the Mg-bearing compounds (Q+ε-Mg_2Si) and Fe-bearing (π+β) intermetallics are provided in Fig. 6 with respect of the Cu content (alloys: Cu0, Cu0.5 and Cu1) and of the solution treatment temperature (S500°C or S530°C).

In order to better display the influence of both heat treatment conditions and Cu addition over the evolution of the different compounds, the area fraction of the phases have been normalized to the total phase area fraction as measured in the as-cast reference sample for each alloy.

The Area Fraction of the phases quantified in the original A356 alloy (Cu0) and in the copper containing alloys (Cu0.5 and Cu1) are presented in Figs. 6a and 6b during the solution treatment at 500°C.

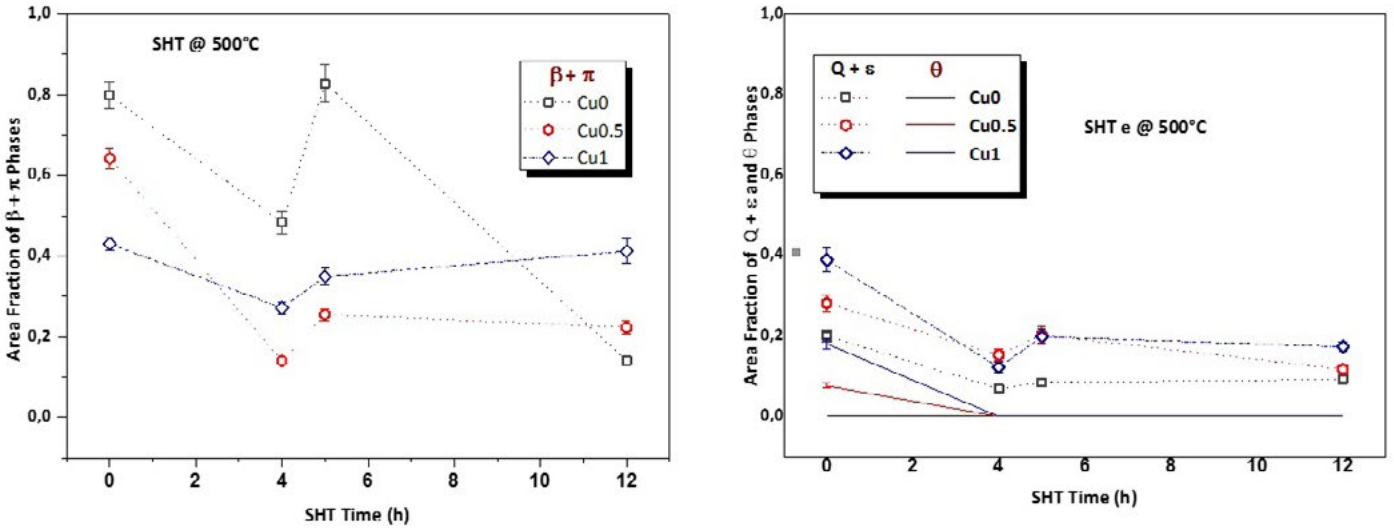

Fig.6 - The quantified area fractions of a) (β+π) phases and b) (Q+ε) and (Θ) intermetallics during Solution Treatment (SHT) at 500°C for different Cu content alloys.

As the Q- and Mg_2Si-phases (marked as Q+ε) appeared in the etched microstructure with more or less the same color (dark – Mg bearing intermetallics), both phases were counted together (Q+ε-Mg_2Si) in image analysis (Fig. 6b). A similar approach has been used for the Fe bearing intermetallics (i.e., π and β) due to their lower contrast in color; these two phases were counted together as well (Fig. 6b).

The area fraction of (β+π) intermetallics decreases in 4 hours and then enhances to a peak in one hour, independently from the Cu content (Cu0, Cu0.5 or Cu1). For longer times, their area fraction converges to values between 0.18 and 0.4. The Cu0.5 sample shows the most significant reduction in area fraction of (β+π) intermetallic after 4h (to 25% of the initial value); moreover, at the end of treatment time (12 hours), the Cu1 sample contains the higher fraction (0.42) of (β+π).

Fig. 6b shows the area fraction variation of Q- and Mg_2Si-phases (Q+ε) and Θ intermetallic phase during solution at 500°C, for Cu0, Cu0.5 and Cu1 samples. As the Q-phase contains Copper ($Al_5Cu_2Mg_8Si_6$), the curve related to Cu0 only includes Mg_2Si. In this case again, after 4 hours treatment, an increase in area fraction, although small (0.02), is observed. Moreover, a quantity of Mg_2Si equal to 0.1 is still present after 12 hours. For Cu0.5 and Cu1 samples, the Q-and Mg2Si-phase area fractions evolve during time presenting a minimum after 4 hours and reaching a stabilisation at 12 hours close to Cu0 value. The Θ phase has already disappeared after 4 hours of solution treatment, regardless of the Cu content.

In order to better understand the intermetallic phase evolution and the solid solution strengthening at 500°C, Vickers microhardness was carefully measured with a load of 5 g in the matrix regions (Fig. 7) where intermetallics or Si particles were not detectable by optical microscopy, for Cu0, Cu0.5 and Cu1 samples. Two behaviours are distinguishable in the graph depending on the amount of Copper present in the alloy. In the Cu0 sample, $HV_{0.005}$ increases by 5 units in 4 hours due to Mg and Si atom solid solution strengthening but, it decreases to the starting value in one hour, retaining the 60HV value until the end of time considered (12 hours). The increase of HV, related to the increase of Mg and Si in solid solution, corresponds to a decrease of (β+π) area fraction at 4 hours (Fig. 5a). Moreover, the subsequent decrease in HV (consistent with a lower content of Mg and Si in SS) determines the area fraction increase of (β+π) phases (as they were counted together it makes sense to think that the contribution to the total area fraction is different between β and π).

In the copper containing alloys, the higher solid solution hardening belongs to Cu0.5, as it reaches the highest HV values after 5 hours. Moreover, hardness has a peak at 5 hours for both Cu0.5 and Cu1 alloys, contrary to what is seen for the Cu0 sample. The presence of Cu in solid solution of course, increases the HV in the matrix but it determines, at the same time, the reduction of Θ to 0% area fraction, regardless of the Cu content. The area fraction of Q+Mg_2Si (Q+ε) phases decreases to 50% of the starting value in 4 hours and afterwards increases to 0.2 area fraction. This value remains quite close to the last detected. From these measurements, the Cu0.5 samples represent the most effective alloy in modifying the kinetics of dissolution/precipitation of the evaluated intermetallics.

According to Fig. 8a, the electrical conductivity (EC) measured after solution treatment at 500°C increases with time for the Cu0, while it decreases for the Cu1 sample. The Cu0.5 has an overall decreasing trend, even if there is a minimum at 4 hours. These EC measurements seem consistent with matrix microhardness shown in Fig. 7.

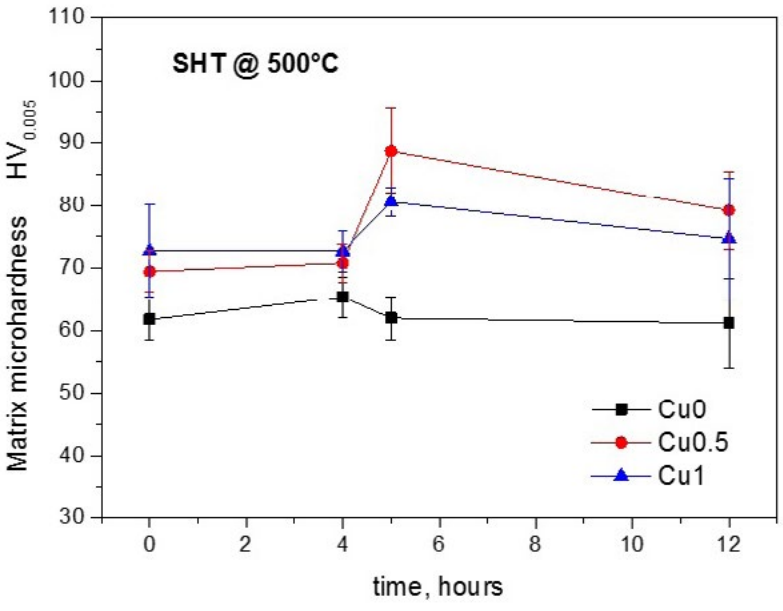

Fig.7 - Matrix microhardness after solution heat treatment at 500°C + natural aging.

The increase in EC for the Cu0 may be the result of the following overall compensation: Mg and Si atoms go in solid solution and -at the same time- are recycled by the intermetallic phase (mainly β and π) by inducing a decrease in the matrix microhardness. For the Cu1 sample, the EC reduction during solution treatment is related to the higher quantity of Cu, Mg and Si atoms that remains in solid solution, as justified by the increase in matrix microhardness.

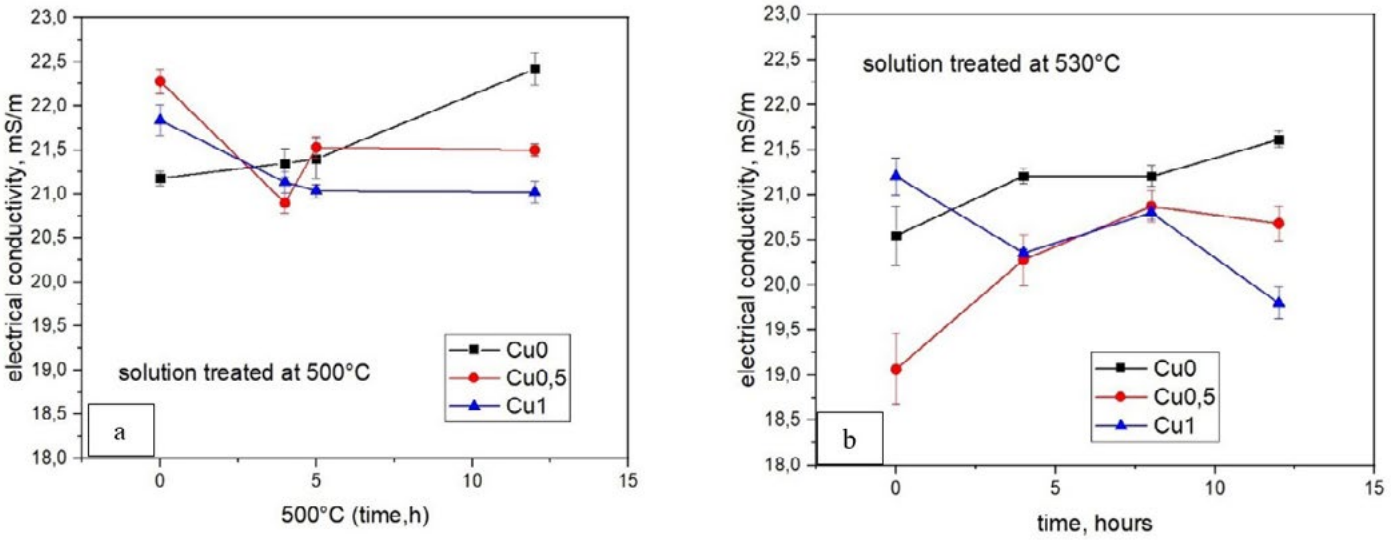

Fig.8 - Electrical conductivity measured after solution treatment and aging at room temperature. a) SHT at 500°C, b) SHT at 530°C.

The EC values measured after the heat treatment at 530°C (Fig. 8b) are generally lower than those at 500°C, as expected from the physical meaning of EC measurements, due to the higher presence of atoms in solid solution at higher temperature. According to the EC trend, the kinetics of solution treatment at 530°C is similar, to the 500°C one for the Cu0 and Cu1 samples. On the contrary, the Cu0.5 sample shows an increase in EC values in relation to time, differently from what emerged at 500°C, where it decreased. The importance of this reversed trend is connected to the effect that the presence of 0.5% Cu has in this matrix (0.5Cu sample). At 530°C, the balance between Cu, Mg and Si atoms that leave the matrix and are caught by the intermetallic phases and those present in solid solution is positive for Cu0.5 sample. Hence, the EC increases and settles in the considered time. This is directly explainable by the stabilization in the area fraction of intermetallic phases present at 530°C for Cu0.5 as it is shown in Figs. 9a and 9b.

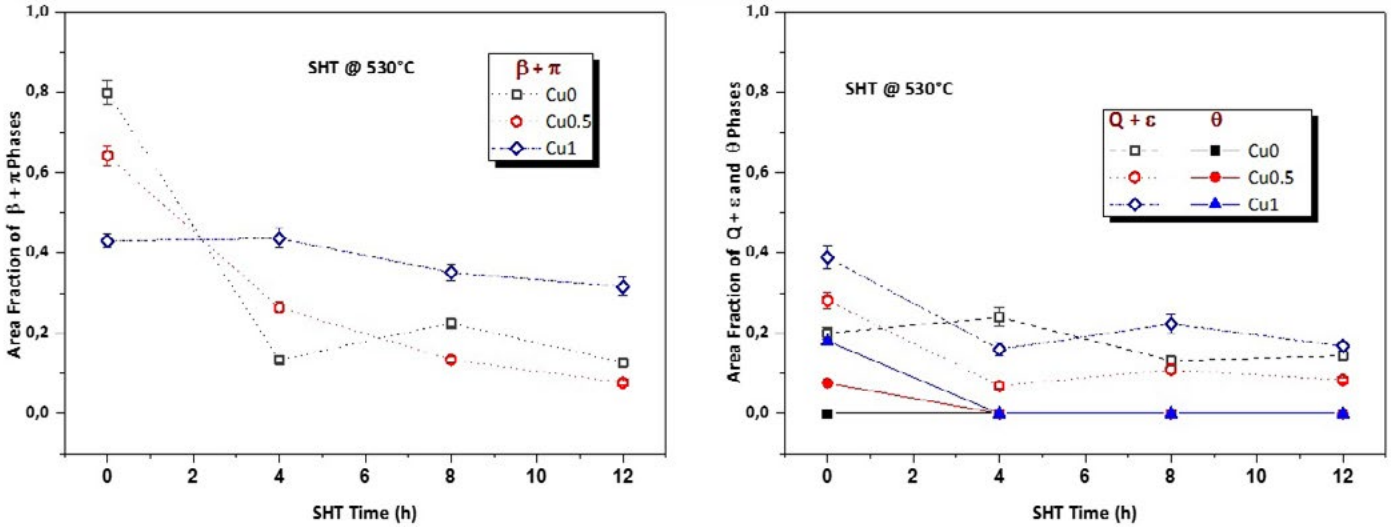

Fig.9 - The quantified area fractions of a) (β+π) phases and b) (Q+ε) and (Θ) intermetallics during Solution Treatment (SHT) at 530°C for different Cu content alloys.

The addition of 1% Cu to the original alloy brings to a stabilization of (β+π) phases (area fraction of 0.4, Fig. 9a) during solution treatment at 530°C, while for lower Cu contents (Cu0 and Cu0.5), samples lose 70% of their (β+π) area fraction. As for the evolution of (Q+ε) intermetallics at 530°C (Fig. 9b), the effect of Cu is similar to Cu0.5 and Cu1 samples with a slight reduction related to time. In the Cu0 sample, where only the ε phase is present (Fig. 9b), the evolution is exactly specular to the Cu containing samples (Cu0.5 and Cu1).

CONCLUSIONS

In this work, the influence of Cu content (0 - 0.5- 1wt%) on the stability of intermetallic phases in a modified A356 aluminium alloy was investigated at 500° and 530°C by optical microscopy, SEM, Vickers microhardness and electrical conductivity. The following conclusions can be drawn:

- The presence of copper modified the stability and the dissolution kinetics of (β+π). At the two investigated solution temperatures, their area fraction decreases with time in Cu0 and Cu0.5 samples. In Cu1 samples, the area fraction of (β+π) remains almost constant with time and comparable at the end of two solution treatments.
- The (Q+ε) intermetallics area fraction increased with copper content (Cu0.5 and Cu1 samples) especially at the highest temperature investigated (530°C); conversely, their area fraction decreased with time. Regarding the Θ phase, it was no more detectable after 4 hours, independently from the Cu content and temperature.
- The measurements of electrical conductivity and matrix microhardness confirmed the overall behaviour during the investigated solution treatments.

AKNOWLEDGEMENTS

Authors wish to thank Hydro Aluminium for original alloy.

REFERENCES

[1] Chakrabarti D.J., Laughlin D.E.: Phase relations and precipitation in Al–Mg–Si alloys with Cu additions, Progress in Materials Science 49, 389–410 (2004).

[2] Cayron C., Buffat P.A.: Transmission Electron Microscopy study of the β' phase (Al-Mg-Si alloys) and QC phase (Al-Cu-Mg-Si alloys): ordering mechanism and crystallographic structure, Acta Mater. 48, 2639-2653 (2000).

[3] Han Y.M., Samuel A.M., Samuel F.H., Doty H.W.: Dissolution of Al2Cu phase in non-modified and Sr modified 319 type alloys, Int. J. Cast Metals Research 21, 371 (2008).

[4] Javidani M.: PhD Thesis Http:// Hdl.Handle.Net/20.500.11794/26146.

[5] Sjölander E, Sefeddine S.: The heat treatment of Al–Si–Cu–Mg casting alloys, J. Mat. Proc. Tech., vol. 210, 1249 (2011).

[6] Crowell N., Shivkumar S.: Solution Treatment Effects in Cast Al-Si-Cu Alloys, AFS Trans., vol. 107, 721 (1995).

[7] Dons A.L., Pedersen L., Brusethaug S.: Modelling the microstructure of heat treated AlSi foundry alloys, Aluminium 76, 294–297 (2000).

[8] Taylor J., St. John D., Barresi J., Couper M.: Influence of Mg content on the microstructure and solid solution chemistry of Al-7% Si-Mg casting alloys during solution treatment, Mater. Sci. Forum, vol.331, 277 (2000).

[9] Rometsch P., Schaffer G.:, Taylor J.: Mass balance characterisation of Al-7Si-Mg alloy microstructures as a function of solution treatment time, Int. J. Cast Met. Res., vol. 14, 59 (2001).

[10] Javidani M., Larouche D.: Application of cast Al–Si alloys in internal combustion engine components, Int. Materials Reviews 59, 132 (2014).

[11] Zheng Y., Xiao W., Ge S., Zhao W., Hanada S., Ma C.: Effects of Cu content and Cu/Mg ratio on the microstructure and mechanical properties of Al–Si–Cu–Mg alloys, J. Alloys Comp., vol. 649, 291-296 (2015)

[12] Yan X., Lin J.C., Us Patent. 0105045 A1. May 2013.

[13] Javidani M., Larouche M., Grant D., Chen X.: Assessment of Post-eutectic Reactions in Multicomponent Al-Si Foundry Alloys Containing Cu, Mg, and Fe, Met. Mat. Trans.A 47, 4818 (2016).

[14] Lasa L., Rodriguez-Ibabe J.M.: Evolution of the main intermetallic phases in Al-Si-Cu-Mg casting alloys during solution treatment, J. Mat. Sci. 39, 1343 (2004).

[15] Di Giovanni M.T., Cerri E., Saito T., Akhtar S., Asholt P., Li Y.J., Di Sabatino M.: How slight solidification rate variations within cast plates affect mechanical response: a study on as-cast A356 alloy with Cu addition Adv. Mat. Sci. Eng. 11, Article Id 4030689 (2018).

[16] Bs Iso 13322-1 (2006) Particles Size Analysis- Image Analysis Methods.

[17] Lattanzi L., Di Giovanni M.T., Giovagnoli M., Fortini A., Merlin M., Casari D., Di Sabatino M., Cerri E., Garagnani G.L.: Room Temperature Mechanical Properties of A356 Alloy with Ni Additions from 0.5 wt.% to 2 wt.%, Metals 8, 224 (2018).

[18] Zhang D.L., Zheng L.: The quench sensitivity of cast Al-7 wt pct Si-0.4 wt pct Mg alloy, Met. Mat. Trans. A27, 3983 (1996).

[19] Kang H.K., Kida M., Miyahara H., Ogi K.: Age-Hardening Characteristics of Al-Si-Cu-Base Cast Alloys, Afs Trans. 27, 507 (1999).

[20] Zafar S., Ikram N., Shaikh M.A., Shoaib K.A.: Microstructure studies in Al – 6% Si – 1.9% Cu – X% Mg alloys, J. Mat. Sci. 25, 259 (1990).

[21] Li Y.J., Brusethaug S., Olsen A.: Influence of Cu on the mechanical properties and precipitation behavior of AlSi7Mg0.5 alloy during aging treatment, Scripta Mat. 54, 99 (2006).

[22] Sivarupan T., Taylor J.A., Cáceres C.H.: Alloy Composition and Dendrite Arm Spacing in Al-Si-Cu-Mg-Fe Alloys, Met. Mat. Trans. A 46, 2082 (2015).